

# Measurement of the six Dimensional Phase Space at the New GSI High Current Linac

P. Forck, F. Heymach, T. Hoffmann, A. Peters, P. Strehl

Gesellschaft für Schwerionenforschung GSI, Planck Strasse 1, 64291 Darmstadt, Germany

e-mail: p.forck@gsi.de

## Abstract

For the characterization of the 10 mA ion beam delivered by the new High Current Linac at GSI, sophisticated, mainly non-intersecting diagnostic devices were developed. Besides the general set-up of a versatile test bench, we discuss in particular bunch shape and emittance measurements. A direct time-of-flight technique with a diamond particle detector is used to observe the micro-bunch distribution with a resolution of  $\sim 25$  ps equals  $0.3^\circ$  in phase. For the determination of the energy spread a coincidence technique is applied, using secondary electrons emitted by the ion passing through an aluminum foil 80 cm upstream of the diamond detector. The transverse emittance is measured within one macro pulse with a pepper-pot system equipped with a high performance CCD camera.

## 1 BEAM DIAGNOSTICS FOR THE LINAC COMMISSIONING

At GSI upgraded ion sources [1] as well as a new 36 MHz RFQ- and IH-Linac designed for high current operation was commissioned in 1999 [2]. New beam diagnostic developments were necessary due to the high beam power up to 1.3 MW at an energy of 1.4 MeV/u within a macro pulse length of maximal 1 ms. A beam diagnostics bench was installed behind each Linac-structure during the step-wise commissioning, the scheme is shown in Fig.1. Non-destructive devices are used for following tasks:

The *total current* is measured using beam transformer [3] made of Vitrovac 6065 core having a  $2 \times 10$  differential secondary winding. The resolution is 100 nA at a bandwidth of 100 kHz. Due to a feedback circuit the droop is less than 1 % for 5 ms macro-pulses.

The *beam energy* is determined by a time-of-flight technique using two  $50 \Omega$  matched capacitive pick-ups [4] with 1 GHz bandwidth, separated by 2 m. A precision of  $\Delta W/W = 0.1 \%$  is achieved.

The *beam position* is monitored by digitizing the power of the  $6^{\text{th}}$  harmonics of the rf frequency (216 MHz) of the 4 segments of these pick-ups.

The *beam profile* is determined by a residual gas monitor [4], where residual gas ions are detected on a 23 strip printed board. For typical beam parameters no significant broadening of the profiles due to space charge influence is expected. For lower current or shorter macro pulses conventional profile grids are used.

The instruments are now installed behind the last IH2 cavity as well as behind the gas stripper. In the following

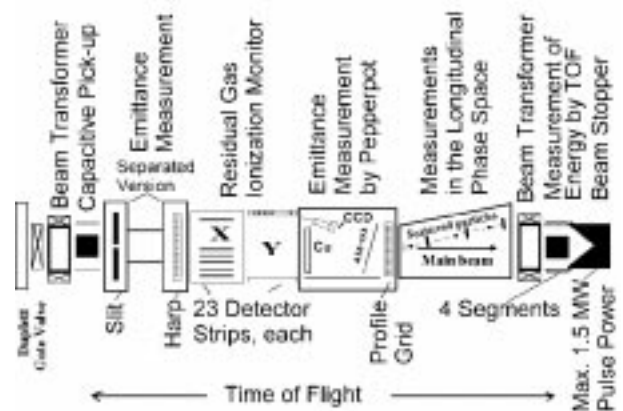


Figure 1: Scheme of the test bench as arranged for the commissioning of the RFQ.

we discuss the measurement in the longitudinal plane using particle detectors and of the transverse emittance using the pepper-pot system.

## 2 MEASUREMENT OF BUNCH STRUCTURE

For the comparison to calculations, as well as for matching of different Linac structures the knowledge of the bunch shape is important, but measurements are not as common as for the transverse case. At velocities much below the speed of light the signal on a transverse pick-up does not represent the details of the bunch shape due to the large longitudinal electric field component. A comparison of the pick-up signal to the bunch shape measured with the method described below is shown in Fig.2 for a velocity of  $\beta = 5.5 \%$  (1.4 MeV/u) to visualize the broadening of the pick-up signal detecting bunches with less than 1 ns width. We developed a device where the arrival of the ion in a particle detector is measured with respect to the accelerating rf, see Fig.3. The method demands for less than one ion hit per rf period. This reduction is done by Rutherford scattering in a  $210 \mu\text{g}/\text{cm}^2$  tantalum foil ( $\sim 130$  nm thickness) at a scattering angle of  $2.5^\circ$  defined by a collimator with 16 cm distance and  $\varnothing 0.5$  mm apertures to give a solid angle of  $\Delta\Omega_{lab} = 2.5 \cdot 10^{-4}$ . The parameters are chosen to get an attenuation of  $\sim 10^{-8}$  of the beam current. A high target mass is preferred, so the energy spread for a finite solid angle is lower than the required resolution. For our parameters the largest contribution to the energy spread arises from the electronic stopping in the foil, which amounts e.g. for Ar projectiles to  $\sim 0.25 \%$  and for U to  $\sim 0.15 \%$  (FWHM)

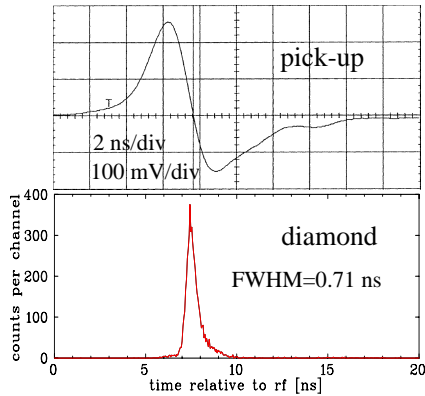


Figure 2: Comparison of a pick-up signal to the bunch shape determination using the particle detector setup for a 1.4 MeV/u  $\text{Ar}^{1+}$  beam 3 m behind the IH2 output. (The 50  $\Omega$  termination of the pick-up leads to a differentiation)

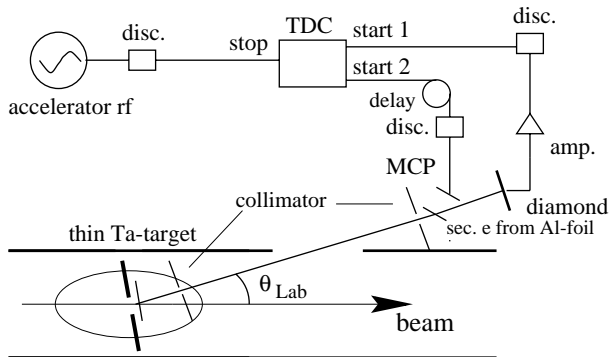


Figure 3: Sketch of the designed TOF method for the bunch shape (Sec.2) and phase space distribution (Sec.3) measurement with particle detectors.

at 1.4 MeV/u. More details can be found in [5].

A drawback of this method is the high sensitivity of the tantalum foil due to the heating by the ions energy loss. Therefore, the beam has to be attenuated, which can be done by defocusing. The device is now installed behind the gas stripper and the first charge separating magnet so that another type of attenuation can be applied by changing the gas pressure or by selecting a different charge state. By this means also space charge effects can be studied.

Another approach would be the use of a supersonic high density Xenon gas target instead of the Tantalum foil; estimations of the effect of the larger elongation have to be done.

After a drift of  $\sim 1$  m the scattered ions are detected by a CVD diamond detector [5, 6]. Besides the very low radiation damage, we gain mainly from the very fast signals, having a rise time below 1 ns. The conversion to logical pulses is done by a double threshold discriminator [7]. The logical pulses serve as a start of a VME time-to-digital converter (CAEN V488), where the stop is derived from the 36 MHz used for accelerating. The timing resolution of the system is about 25 ps corresponding to a phase width of  $0.3^\circ$ .

As an example, the bunch structure of a 120 keV/u  $\text{Ar}^{1+}$  beam at the output of the Super Lens (and an additional

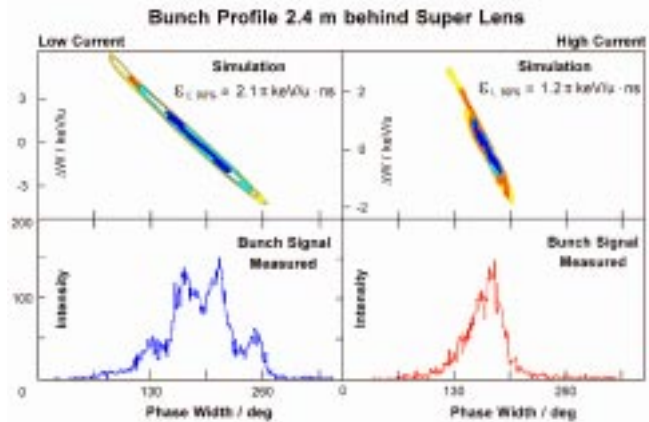


Figure 4: Example of the bunch shape measurements 2.4 m behind the Super Lens. On the left bottom the result for a low current 0.1 mA  $\text{Ar}^{1+}$  beam is shown, on top the calculated emittance is plotted. On the right the measurement and simulation are shown for a high current of 5 mA  $\text{Ar}^{1+}$ .

drift of 2.4 m) is shown in Fig.4. The two measurements for low (left) and high (right) current show a quite different bunch shape having a larger, filamented emittance for the low current case. The particle tracking calculation [8] shows a strong ion current dependence for the longitudinal emittance. The applied rf power in the cavity counteracts the space charge force for a high current beam. For a low current filamentation occurs due to the missing damping by the space charge. Other experimental results can be found in [2].

### 3 MEASUREMENT OF LONGITUDINAL EMITTANCE

The main advantage of using particle detectors is the possibility to measure the longitudinal emittance using a coincidence technique. As shown in Fig.3, a second detector can be moved in the path of the scattered ions. It consists of a  $15 \mu\text{g}/\text{cm}^2$  Aluminum foil ( $\sim 50$  nm) where several secondary electrons per ion passage are generated. These electrons are accelerated by an electric field of 1 kV/cm towards a micro channel plate equipped with a 50  $\Omega$  anode (Hamamatsu F4655-10). The time relative to the accelerating rf is measured as well as the arrival time of the same particle at the diamond detector located 80 cm behind the MCP. From the difference in time of the *individual* particles one can generate a phase space plot.

An example of such a measurement is given in Fig.5 (left) for a low current Ar beam 2.5 m downstream of the gas stripper. The arrival times at the diamond detector are used as the phase (or time) axis having a width of 1.4 ns equals  $18^\circ$  phase width. The time difference between diamond and MCP is plotted at the y-axis, the width is about 0.4 ns (FWHM) corresponding to an energy spread of  $\Delta W/W = 1.7\%$ . For a high current beam (5 mA before stripping) a double structure is visible in the bunch profile and an energy broadening to  $\Delta W/W = 2.8\%$  with a clear correlation in the phase space. Here the attenuation is

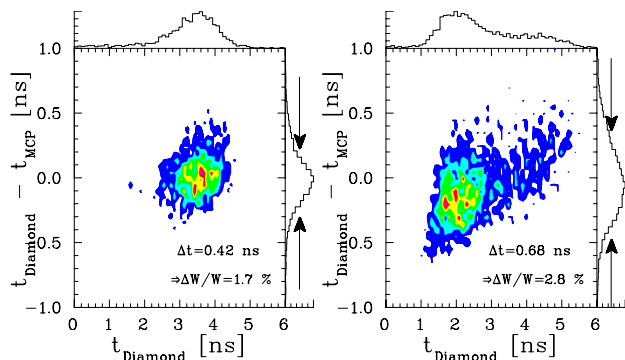


Figure 5: Measured longitudinal phase space distribution for a low current Ar-beam (left) and a high current beam (right) 2.5 m behind the stripper. Note that the measured energy spread might be too large.

done by selecting a high charge state ( $\text{Ar}^{15+}$ ) far from the maximum of the stripping efficiency curve ( $\text{Ar}^{10+}$ ). The measured values are larger by a factor of 2 as expected by tracking calculation. Therefore it is believed that some errors contribute to the measurement: Having a drift length of only 80 cm between the two detectors and an ion velocity of 5.5 % of the ions (corresponding to 48 ns time of flight) the accuracy in time has to be 25 ps to have a precision of  $\Delta W/W$  of 0.1 %. The imperfections of the device, in particular the lack of homogeneity of the accelerating field for the electrons towards the MCP effect the resolution in time. An optimization has to be done. A large distance (e.g. 3 m) between the two detectors would lower the requirement for the time resolution of the detectors. Recently it was discovered that there might be some problems inside the stripper [2] due to inhomogeneity of the gas jet resulting in a wider energy spread as the design value.

It is shown, that this type of setup can be used for the determination of the longitudinal emittance at low ion velocities, but a careful design of the components is necessary.

#### 4 MEASUREMENT OF TRANSVERSE EMITTANCE

For the measurement of the transverse emittance two devices were installed at the diagnostic bench. A conventional slit-grid system [4] having a coordinate resolution of 0.05 mm and an angular resolution of 0.3 mrad. Due to the high beam power, this device can only be used for the lower energy part of the Linac. For high current operation we developed a pepper-pot system capable to measure the emittance within one macro-pulse, see [9] for more details. Here the coordinates are fixed by a  $45 \times 45 \text{ mm}^2$  copper plate equipped with  $15 \times 15$  holes with  $\text{Ø}0.1 \text{ mm}$ . After a drift of 25 cm the beam-lets are stopped on a  $\text{Al}_2\text{O}_3$  screen. The divergence of the beam is calculated with respect to the image of the pepper-pot pattern. This image is created on the screen with a HeNe laser, which illuminate the pepper-pot via a pneumatic driven mirror. This calibration eliminate systematic errors due to mechanical uncertainties. A

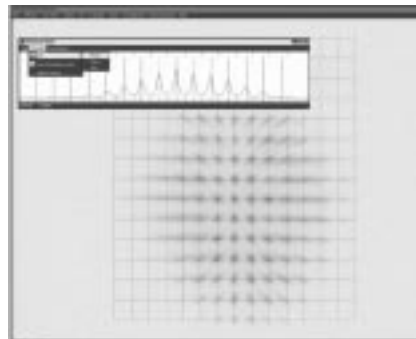


Figure 6: Screen shot from the pepper-pot device for an Ar beam and, as an insert, the projection onto the horizontal plane.

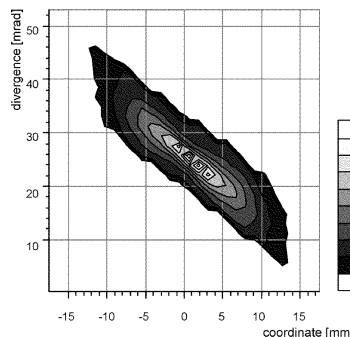


Figure 7: Phase space plot of the data shown above.

high resolution 12 bit CCD camera (PCO SensiCam) transmits the digital data via fiber optics. A typical image of such a measurement is shown in Fig.6, together with the projection onto the horizontal or vertical axis. This projection is used for the emittance calculation with an algorithm like for the slit-grid device.

For a precise measurement the beam width should be large enough to illuminate several holes in the pepper-pot plate (spacing 3 mm). This also avoids overheating of the pepper-pot, as well as saturation of the light intensity emitted from the screen. In addition, a background level (about 5 %) has to be subtracted from the data, probably caused by scattered light in the screen. Therefore the beam optics have to be changed in some cases to use this modern and reliable system for a fast measurement in a high current operation.

#### 5 REFERENCES

- [1] H. Reich, P. Spätke and L. Dahl, P. Spätke, this proceedings
- [2] W. Barth and W. Barth, P. Forck this proceedings
- [3] N. Scheider, AIP proceedings 451, p. 502 (1998).
- [4] P. Forck, A. Peters, P. Strehl, AIP proceedings of the Beam Instrumentation Workshop, Boston (2000).
- [5] P. Forck et al., proceedings of the 4<sup>th</sup> DIPAC, Chester, p. 176 (1999).
- [6] E. Berdermann et al., *Proc. XXXVI Int. Winter Meeting of Nucl. Phys., Bormio* (1998).
- [7] C. Neyer, 3<sup>rd</sup> Workshop on Electronics for LHC Experiments, London, CERN/LHCC/97-60 (1997).
- [8] A. Schempp, LINAC 96, proceedings, Geneva (1996).
- [9] T. Hoffmann et al., AIP proceedings of the Beam Instrumentation Workshop, Boston (2000).